

**Paper for the Special Session on Nanostructured Materials at the 45th
AIAA/ASME/ASCE/AHS/ASC
Structures, Structural Dynamics and Materials Conference and Exhibit**

**Stress Distribution During Deformation of Polycrystalline Aluminum by Molecular-Dynamics
and Finite-Element Modeling**

V. Yamakov*, E. Saether†, D. Phillips‡ and E.H. Glaessgen†
NASA Langley Research Center, Hampton, VA 23681, U.S.A

Abstract

In this paper, a multiscale modelling strategy is used to study the effect of grain-boundary sliding on stress localization in a polycrystalline microstructure with an uneven distribution of grain size. The development of the molecular dynamics (MD) analysis used to interrogate idealized grain microstructures with various types of grain boundaries and the multiscale modelling strategies for modelling large systems of grains is discussed. Both molecular-dynamics and finite-element (FE) simulations for idealized polycrystalline models of identical geometry are presented with the purpose of demonstrating the effectiveness of the adapted finite-element method using cohesive zone models to reproduce grain-boundary sliding and its effect on the stress distribution in a polycrystalline metal. The yield properties of the grain-boundary interface, used in the FE simulations, are extracted from a MD simulation on a bicrystal. The models allow for the study of the load transfer between adjacent grains of very different size through grain-boundary sliding during deformation. A large-scale FE simulation of 100 grains of a typical microstructure is then presented to reveal that the stress distribution due to grain-boundary sliding during uniform tensile strain can lead to stress localization of two to three times the background stress, thus suggesting a significant effect on the failure properties of the metal.

Introduction

Uneven stress distribution and stress localization during deformation are the key factors for fracture and failure in polycrystalline metals. The inhomogeneous polycrystalline microstructure that consists of grains of different size and shape joined together at different angles and forming various types of grain-boundaries (GBs) creates inhomogeneous deformation fields at, otherwise,

homogeneous loading. There are a number of factors responsible for the appearance of inhomogeneous deformation inside the polycrystal. The co-existence of grains of different size and orientation with anisotropic elastic properties is one factor. The difference in the structure and properties of the GBs between grains of various misorientations is a second factor for uneven stress distribution. A third factor is grain-boundary sliding (GBS), i.e., the rigid translation of one grain relative to another at the GB interface. When grains deform, GBS is an inevitable process as a result of the relative movements and rearrangements of the grains¹. GBS is a strongly inhomogeneous mode of deformation localized at a very narrow interface layer thus creating very strong shear forces. This, together with the fact that the shear strength of a general GB between grains of high misorientation angle (high-angle GB) is much lower than the shear strength of the perfect crystal^{2,3} leads to GBS being an efficient deformation mode. During GBS the load transfer between the sliding surfaces is significantly reduced and the load is redirected to other places more resistant to sliding. This sliding creates redistribution of the load and appearance of stress localization in the microstructure which, in the absence of an efficient accommodation mechanism, can lead to void formation and microcracking.

In this paper, a multiscale modelling strategy is used to study the effect of GBS for stress localization in a polycrystalline microstructure. Although they reveal the system behavior at atomic level resolution, MD calculations of large systems of grains are computationally prohibitive to perform, and a more efficient analysis technique is sought. Finite element method (FEM) analysis is an obvious choice, however, the FEM models cannot a-priori simulate the deformation mechanisms found within the systems of grains. Thus, the FEM models must be tuned in order to reproduce the stress localization observed in the atomistic simulations. For this purpose, a polycrystalline model of bimodal grain-size distribution

*National Institute of Aerospace

† Analytical and Computational Methods Branch, Member AIAA

‡ Lockheed Martin Space Operations, Member AIAA

was constructed convenient to study by both, MD and FEM simulations. The MD simulations revealed the behavior of this model with atomic-scale details. Additional MD simulations on a bicrystal model were performed to extract the elastic and yield properties of the GBs presented in the model. These GB properties were then used to tune the FEM model to reproduce closely the behavior of the test model to match with the MD simulation results. The FEM model can then be used as part of a multiscale modelling strategy to extrapolate the MD-derived information to larger scales to study the failure properties of polycrystalline materials.

The paper is constructed as follows. First, details of the configuration model used in both, MD and FE simulations are discussed. The specific features of the MD model are presented next. Further, the yield strength of the GB is defined by using MD simulations on a bicrystal. This yield strength is used as an input parameter to the FEM model. Next, the FEM version of the model is discussed and the results of the FEM simulation are compared with those from the MD simulation. Finally a large-scale FEM simulation of a typical microstructure of 100 grains is analyzed to reveal the stress distribution due to grain-boundary sliding in a more general polycrystalline system.

The Configuration Model

To investigate the effect of GBS on the stress distribution in a polycrystal of inhomogeneous grain size a configuration model, presented in Figures 1(a) and (b) was used. This configuration was used in both, MD and FEM simulations with the additional goal to tune the parameters of FEM to reproduce as close as possible the MD simulation. The model is a periodically repeating unit of a four-grain octagon-square configuration which, when replicated in x - and y -directions represents a polycrystal of a bimodal grain-size distribution. The advantages of this configuration are the following: (i) the model allows exploration of the effect of large variations in the ratio, $a:b$, between the grain sizes (Figure 1(b)), which for this study was set to 1:4; (ii) the model is both simple enough to allow for MD simulation, and informative enough to be used in the FEM simulation to compare with the MD results; (iii) the configuration has a four-fold symmetry (against 90° rotation) which further simplifies the analysis. In both, MD and FEM simulations, this configuration is deformed by applying stress or strain, respectively, along the x -direction. The deformation conditions are chosen such that the grains deform elastically while the GBs deform plastically by GBS. While in the MD model, an interatomic potential representative for aluminum (Al) is used, to isolate the effect of crystal anisotropy on the stress distribution an isotropic media is used for the FE simulation. Though this would result in some inevitable discrepancy in the results, it would help to identify the amount of stress distribution due to GBS alone. Fixed boundary conditions, shown in Figure (b), which for an isotropic

media mimic the periodic boundary conditions in the MD simulation, shown in Figure (a), were applied in the FE simulation.

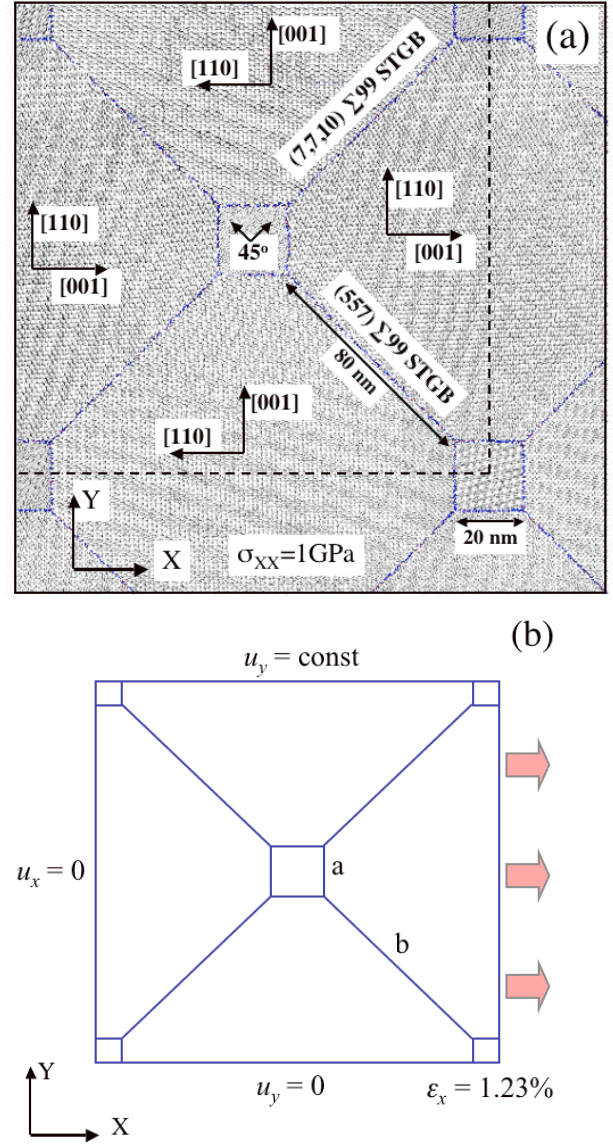


Figure 1: (a) A snapshot of the thermally equilibrated polycrystalline microstructure designed to study the effect of GBS on the stress distribution in a polycrystal of bimodal grain-size by MD simulation. The GBs are shown as darker (blue) lines of atoms which were identified to be in disordered (non-crystalline) local environment. The dashed lines mark the actual system-box dimensions while, for better visualization the microstructure is slightly extended using periodic boundary conditions. (b) Repeating unit used in FE simulations to model grain structure shown in (a). As there is no characteristic length-scale in the FE model, the dimensions in (b) are relative, characterized by $a:b = 1:4$ consistent with (a).

The Molecular-Dynamics Model

To investigate the effect of GBS on the stress distribution in a polycrystal of inhomogeneous grain-size, atomistic MD simulations were used where the only predefined input quantity is the interactive potential between individual atoms which, following Newtonian dynamics, defines their motion. Embedded-atoms-method (EAM) many body potential⁴ fitted to reproduce closely the elastic and thermodynamic properties of a perfect Al crystal was applied. A textured or columnar microstructure model with periodic boundary conditions in all three dimensions to mimic bulk conditions⁵ was ideal for this study. While providing a fully three-dimensional (3d) treatment of the underlying physics, this model makes possible to simulate relatively large grains, because only a few lattice planes need to be considered in the periodically repeated texture direction. The texture z -axis is along [110] crystallographic orientation which enables a realistic dislocation-slip dynamics along six available slip systems in two {111} slip planes in each grain⁶. These slip systems are adequate to accommodate any two-dimensional deformation in the x - y plane of the simulated structure. The grain-boundaries, formed between the grains in this model are [110] tilt GBs which have been studied extensively in the past 15 years both, experimentally⁷⁻¹⁰ and by simulations^{9,13}. In spite of some drawbacks inherent in this model when compared to a fully 3d structure, as discussed in reference 14, the model was proven remarkably successful in predicting the highly unexpected deformation twinning in nanocrystalline Al^{15,16}, and the transition from partial to perfect slip in nanocrystalline fcc metals^{6,15}. Both of these phenomena have since gained a solid experimental support¹⁷⁻¹⁹.

Specifically for this study, a four-grain octagon-square configuration was used as a test model. A snapshot of the microstructure after thermal equilibration at 100 K is given in Figure 1(a). The configuration represents a periodically repeating unit of large octagonal grains of size, $b = 80$ nm, encapsulating small square grains of size, $a = 20$ nm. The thickness of the system in the texture direction was set equal to 5(1,1,0) atomic planes (1.43 nm), as in the previous columnar models^{5,6,15,16}. Within these dimensions, the system contains 1.7 million atoms. By rotating one of the two octagonal grains at 90° relative to the other (the crystallographic orientations are given in Figure 1) the four 45° inclined diagonal GBs become 90° \square 99 symmetric-tilt GBs (STGB) for which the atomic structure in Al is known from the literature¹⁰. The two types of \square 99 STGBs with (5,5,7) and (7,7,10) GB plane, (see Figure 1(a)), are structurally very similar and practically undistinguishable from the point of view of their mechanical properties, which preserves the four-fold symmetry (against 90° rotation) of the structure. In addition, the two small square grains are rotated at 45° relative to the large grains thus forming high-angle asymmetric tilt GBs^{7,8} (Figure 1(a)).

To initiate GB sliding the microstructure was loaded with uniform tensile stress of 1 GPa along the x -axis in Figure 1(a). The stress was applied using Parrinello-Rahman²⁰ constant-stress technique combined with Nose-Hoover thermostat²¹ for constant-temperature simulation. This stress is well below the threshold stress of about 2 GPa^{6,14} needed to start nucleation of dislocations from the GBs, which are the only possible dislocation sources in grains of a nanometer size^{14,15}. Thus, the dislocation activity, as a possible accommodation mechanism was readily suppressed. By running the simulations at very low temperature of 100 K (a value still high enough to avoid quantum-mechanical effects existing in a real structure that cannot be captured by the classical MD technique) GB diffusion, as another possible accommodation mechanism, was also eliminated. Also, low temperature prevents grain-growth, a process which otherwise will be very strong in such a system of a bimodal grain-size distribution. Restricting the dislocation activity and GB diffusion helps to map the MD model better to our FEM simulations which, at the present stage, do not include these mechanisms.

During loading the system reached an equilibrium strain of 1.23%. The strain was elastic within the grains and plastic at the GBs thus initiating GB sliding. At this stage, to present the stress distribution in the system, two-dimensional stress-maps were created. The two-dimensional resolution of the maps is an area of 6x6 lattice parameters (2.43 x 2.43 x 1.43 nm³ volume including 432 atoms) over which the local stress has been averaged. The stress maps were stored every 1 ps over a period of 20 ps after reaching equilibrium (approx. 40,000 MD steps) and then averaged in time to smooth out the fluctuations always present in a system of such small size. These averaging procedures in space and time give a good estimate of the local stress calculated by the virial-expansion technique in Parrinello-Rahman stress-calculation²⁰. All the stress-maps for the three stress components in the x - y plane of deformation (i.e., normal to the texture z -axis), \square_{xx} , \square_{yy} and \square_{xy} , show distinctive stress distribution and stress localization which were then compared with an FEM simulation of the same configuration, as will be discussed below.

Shear strength of a grain-boundary

Knowledge of the shear strength of the GBs presented in the system is crucial for understanding the stress distribution due to GBS. This shear strength is also required as an input for the FEM model discussed below. For this purpose, a separate MD simulation of a bicrystal cubic system, presented in Figure 2, was used. The same interatomic potential⁴ as in the octagon-square model was applied.

The two crystals were crystallographically oriented in such a way as to form a (7,7,10) \square 99 STGB (Figure 2). This type of GB, together with the very similar (5,5,7) \square 99 STGB, were expected to take most of the GBS in the octagon-square model (Figure 1) due to the

maximum resolved shear stress on the planes inclined at 45° to the tensile direction. In the simulation, the system box with periodic boundary conditions was allowed to shear in all three directions in addition to expansion or contraction making it possible to estimate the shear strain directly. The system was loaded with a symmetric shear stress ($\sigma_{xy} = \sigma_{yx}$) to prevent torque forces and to initiate GBS in the direction consistent with the sliding direction between the octagons in the octagon-square model. In addition, a control simulation was performed on a perfect crystal of the same size and orientation ($[5,5,7]/[7,7,10]/[1,1,0]$) to obtain the shear strain of a perfect crystal under the same simulation conditions. The perfect-crystal strain was then subtracted from the bicrystal strain and the resulting strain, due to the GB alone, is presented in Figure 3 as a function of load for three different temperatures.

Following Schiotz et al.²² the yield stress was defined as the stress where the strain starts to depart from linearity, a definition convenient for use in MD simulations. For the temperature of $T = 100$ K, used in the simulation of the octagon-square model, the obtained yield stress is $\sigma_y = 0.2$ GPa. As expected, the yield stress decreases with increasing the temperature of the system becoming 0.14 GPa at 200 K and 0.12 GPa at 300 K. For comparison, the theoretical shear strength of a perfect Al crystal was estimated at around 2.8 GPa²³. Thus, the GBs are shown to be more than an order of magnitude weaker to shear than the perfect crystal grains. Applying a tensile load of 1 GPa along the x-axis in the octagon-square model (Figure 1(a)) results in a resolved shear stress of 0.5 GPa along the diagonal $\{99\}$ GB planes. This stress is more than twice as large as the GB yield stress, as defined here (see Figure 3), but still well below the shear strength of the perfect crystal. This ensures a regime of deformation where the GBs would experience plastic sliding, while the crystal grains would deform elastically.

FEM simulation

For the finite element simulations, a code “FRANC” developed at Cornell University²⁴ was used and specifically designed to study crack initiation and propagation in metallic polycrystals with explicit representations of grains and grain boundaries. Each of the grains in the model was given isotropic, elastic material properties. The properties used were Young’s modulus, $E = 74.8$ GPa, and Poisson’s ratio, $\nu = 0.346$. These values were calculated averages²⁵ from the anisotropic elastic constants of the interatomic potential⁴ used in the MD approach. To accurately account for the entire structure, a repeating unit, similar in geometry to the one used in the MD simulation was chosen (Figure 1(b)). As in the MD model, the ratio of the lengths of the grain boundaries is $a:b=1:4$. Periodic boundary conditions are necessary to accurately compare results to those obtained from MD simulations. The boundary and loading conditions shown in Figure 1(b) are consistent with periodic boundary conditions for an isotropic material

In this work, cohesive zone models (CZM) were used to characterize grain boundary behavior²⁶. Cohesive zone models assume cohesive interactions of the material around a grain boundary and permit the appearance of fracture surfaces in a continuum²⁷. To simulate the sliding behavior along grain boundaries, two independent cohesive zone models are chosen for the normal and shear components of the traction and displacement. To permit sliding, a perfectly plastic relationship is chosen for the shear model with yield stress of 0.2 GPa; this stress is consistent with the numbers obtained from the MD criterion discussed previously. To restrict opening, the normal CZM is specified as having linear elastic behavior with high stiffness. The analysis is performed for 1.23% applied strain. This applied strain corresponds to the 1 GPa applied stress in the MD simulations.

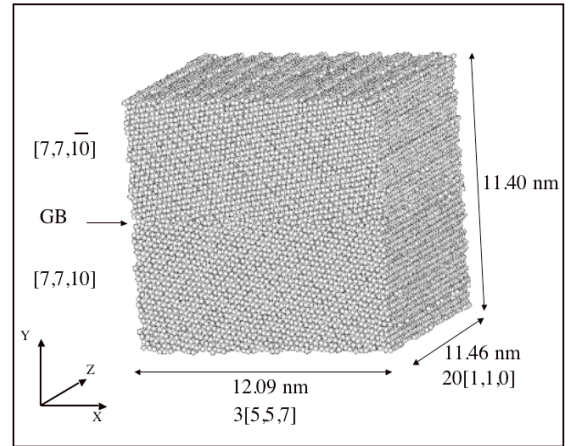


Figure 2: Bicrystal cubic microstructure used to get the shear strength of $\{99\}$ STGB formed in the octagon-square system shown in Figure 1.

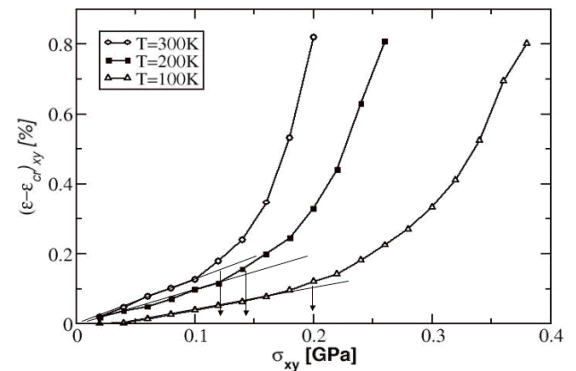


Figure 3: GB shear strain vs stress extracted from the bicrystal model shown in Figure 2. The straight lines, tangential to the curves at their origin, help to mark the linear elastic regime. The arrows show the yield stress for each of the three simulated temperatures defined²² as the stress where the strain starts to depart from linearity.

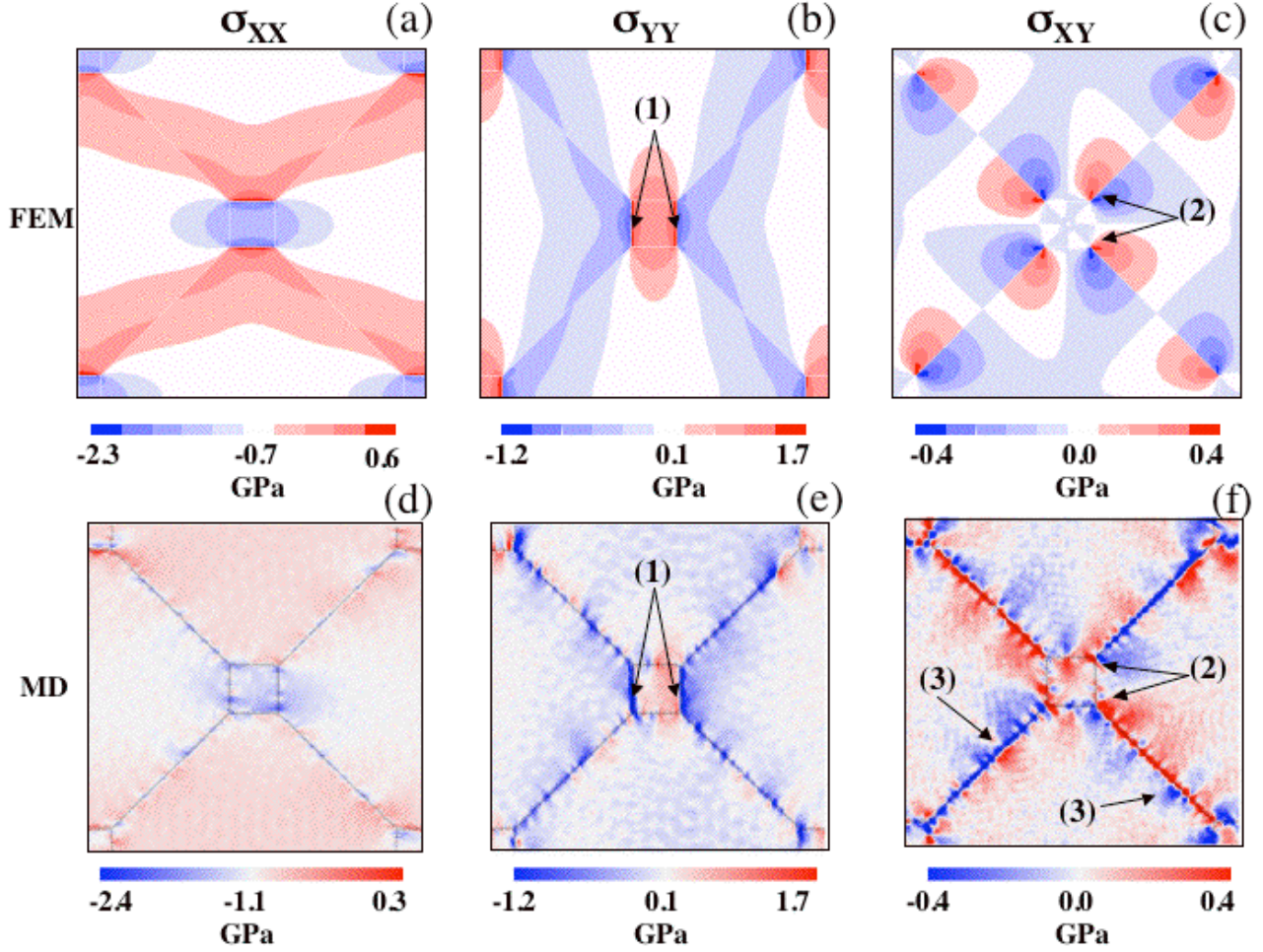


Figure 4: (a-c) Stress contours from the FEM model and the corresponding stress maps (d-e) from the MD model for σ_{xx} , σ_{yy} , and σ_{xy} stress components. Positive and negative stress are indicated in red and blue, respectively, relative to the average background stress defined as white. In (a), (b), (d) and (e) positive stress is defined as the stress in compression and negative as the stress in tension compared to the background stress. In (c) and (f) positive and negative shear corresponds to shear directions at the diagonal GBs defined by Figure 5. The stress localization of σ_{yy} at the GBs of the small grain, marked with (1) in (b) and (e) are significant. Marked with (2) in (c) and (f) are also the shear stress concentrations created at the triple junctions. A few GB dislocations that appeared in the MD simulation and which create disturbances in the GB stress field are indicated with (3) in (f).

Results

Applying a uniform tensile stress of 1 GPa creates resolved shear stresses larger than the GB yield stress, but lower than the yield stress of the grains, producing plastic sliding at the GBs and elastic deformation in the grain interiors. GBS reduces the load transfer from one grain to another and redistributes the stress. The σ_{xx} , σ_{yy} , and σ_{xy} stress distributions for the octagon-square model are shown in Figures 4(a-f). The results from the FE simulations Figures 4(a-c) are compared with the stress maps obtained from the MD simulation Figures 4(d-f). Both models show that the small square grains take most of the load produced from the tensile stress (see Figures 4 (a) and (d)) and from the Poisson contraction perpendicular to the tensile x-direction (see Figures 4 (b) and (e)). This contraction creates a strong tensile stress at

the sides of the square grains normal to the tensile direction (regions marked (1) in Figures 4 (b) and (e)). The close similarity between MD and FEM stress distribution and the fact that the FEM model was isotropic indicates that this stress distribution is solely due to GBS. Through GBS the grains become decoupled in their elastic deformation. At the GBs, where only two grains meet, this decoupling creates sliding, but at the triple junctions where three grains meet strong incompatibility stresses are produced. This is seen in both FEM and MD results (Figures 4 (c) and (f)).

The most direct evidence for the presence of GBS is seen on the MD σ_{xy} -stress map in Figure 4 (f). The four diagonal GBs showed strong shear stress in the two opposite directions (with stress values presented in red and blue). Figure 5 gives a schematic representation of the grain sliding responsible for the observed shear stress

distribution. Grains (1) and (3) are displacing towards each other compressing the small grain (5) in the y -direction, while grains (2) and (4) are displacing apart and stretching grain (5) in the x -direction. The displacement of the large grains results in sliding at the GBs, schematically shown in Figure 5 as couples of oppositely directed arrows on both sides of the diagonal GBs. The direction of each arrow corresponds to the local displacement of each grain at the GB. This displacement produces strong local shear stress at the diagonal GBs as seen in Figure 4(c,f).

In spite of the overall good match between the stress distribution from MD and FEM simulations, there are also significant mismatches that can be discovered after a careful examination of Figures 4(a-f). For example, in the MD simulation there is no full symmetry of the stresses produced on the two small grains, and there are some deviations in the stresses on the large grains too (most pronounced in Figure 4(d)). Possibly, the main reason for these deviations is the small, but noticeable anisotropy in the MD model which results from the interatomic potential. This potential was fitted⁴ to reproduce closely the elastic constants, including the anisotropy, of monocrystalline Al. An anisotropic FEM simulation with the proper periodic boundary conditions is needed to get better comparison.

Another source of mismatch between the two models is the inevitable existence of GB dislocations in the MD model. In a polycrystalline MD model, absolutely perfect GBs are impossible to sustain during loading, even if they were produced initially. The same is true for a real material, but at this stage GB dislocations are not considered in the FEM model. The GB dislocations have long-range elastic fields that can significantly modify the stress distribution in close proximity to the GBs thus altering it from the FEM result. Such an effect produced by GB dislocations is marked as (3) in Figure 4(f). Also, the phonon waves, always existing in finite temperature MD simulation, create periodic modulations in the MD stress maps Figures 4 (d-f) which are non-existent in the FEM stress distributions (Figures 4 (a-c)). Even averaging of the stress over 20 ps time interval was not enough to smooth these fluctuations enough. One reason may be that the periodic boundary conditions imposed on the system, together with its high configuration symmetry, create stationary waves which cannot be smoothed out over such a short period of time. All these factors make the MD maps shown in Figure 4 much more rich and complicated compared to the substantially more idealized FEM results.

The close quantitative match between the stress distribution obtained from MD and FEM simulations of the octagon-square configuration (Figure 4) gives confidence that implementing the properly parameterized CZM elements in the FEM model correctly reproduces GBS for a polycrystalline specimen. With this confidence, FEM can now be used to simulate a typical polycrystalline structure. For this purpose, a sample with

100 randomly shaped and sized grains, represented by Voronoi polygons²⁸, was constructed. The grain configuration, along with the boundary and loading conditions, are shown in Figure 6.

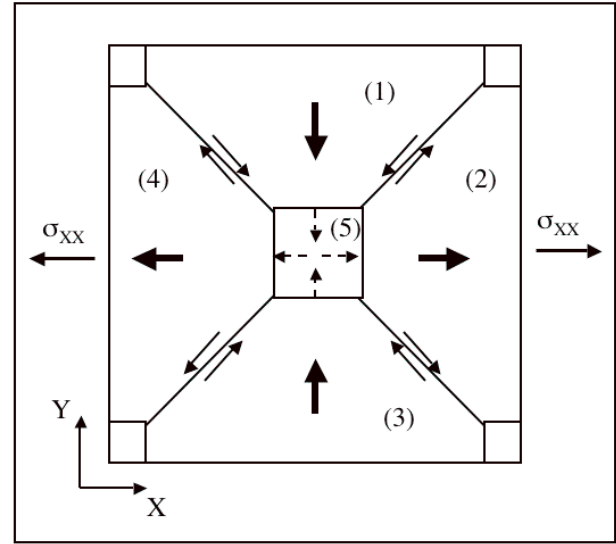


Figure 5. A schematic representation of the sliding directions of the four octagonal grains (bold arrows) and the inserted stresses on the small square grain in the middle (dashed arrows). The local displacements of the material at the GBs, producing GBS are presented by couples of opposite pointing arrows on both sides of the boundaries.

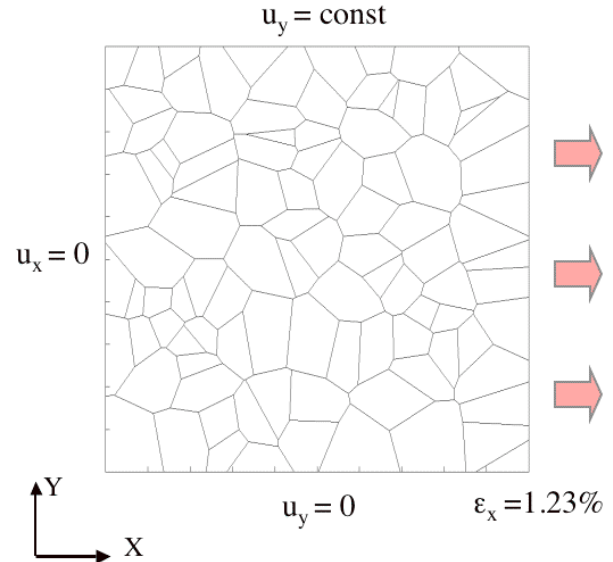


Figure 6: Material model with 100 randomly shaped and sized grains represented by Voronoi polygons²⁸.

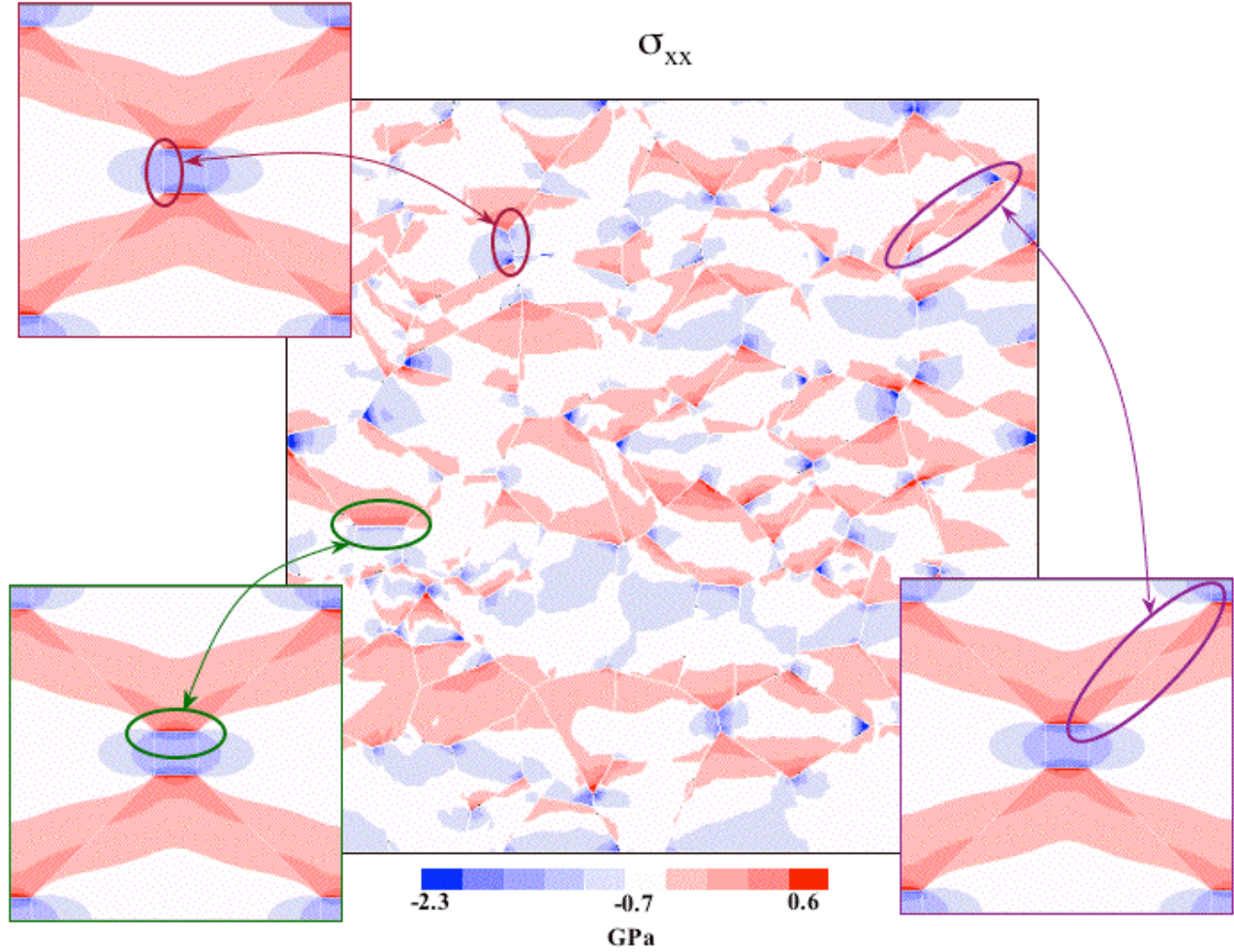


Figure 7: Stress contour σ_{xx} for 100-grain material subjected to 1.23% strain, as shown in Figure 6, with some similarities to the idealized model highlighted.

For 1.23% applied strain, the σ_{xx} stress distribution is shown in Figure 7. The similarities in grain boundary behavior between the randomly configured model and the idealized octagon-square configuration are highlighted. This larger-scale simulation shows that stress localization due to GBS are common within the polycrystals and local stress can exceed several times the background stress, thus marking spots for a possible crack nucleation. It is not surprising²⁹ that these stress concentrations are mostly localized at the triple junctions where three GBs meet.

Summarizing the results from this section, it was shown that simulating the behavior of geometrically identical polycrystalline structures by MD and FEM techniques can serve two purposes. First, it helps to tune the parameters of the larger-scale FEM simulation to the results from the lower-scale MD simulation, thus incorporating the effects of atomistic mechanisms, presented in MD, into a continuum model. Second, such a parallel use of two very different techniques can help to identify more unambiguously the underlying mechanism behind a certain phenomenon. In the presented study,

reproducing a stress distribution by isotropic FE simulation similar to the one obtained from MD simulation where anisotropy is inherent from the interatomic potential and cannot be turned off, proves that GBS played the major role in this case. As a result, it was shown that even in a material of weak anisotropy, such as Al, substantial stress localization can be produced due to GBS.

Concluding Remarks

In the presented study a combined implementation of two modelling techniques, MD and FEM, has been demonstrated working at different length-scale resolutions on two geometrically equivalent systems. The results, after comparing these two simulations, are very instructive. First, a method was successfully applied to match the parameters in the constitutive equations (in this case the CZM) used in the FEM model with quantities extracted from the MD simulation (like GB yield stress). By this method the FEM was

tuned to the MD simulation. Second, in an MD simulation where the resolution is at the level of individual atoms, it is usually very difficult to identify unambiguously the underlying mechanism responsible for a given process. By reproducing the MD simulation experiment by FEM model, where the mechanisms are implemented through constitutive equations and can be easily controlled, the underlying mechanism can be revealed with higher certainty. For example, in the octagon-square model, presented here, the stress distribution obtained by MD simulation cannot be attributed readily to GBS, as there is also anisotropy which can produce analogous effects. After reproducing the similar simulation experiment by FEM using isotropic material parameters, but allowing for GBS with the equivalent sliding resistance as in the MD model and comparing the results it becomes possible to identify what part of the stress distribution is due to GBS alone, and what part is due to other sources like anisotropy and GB dislocations.

In this study it has been also demonstrated that now, because of the advanced computational technology, high-end MD simulations can overlap well with FEM simulations on yet small, but still informative enough systems to allow direct comparison of the results. This possibility suggests a new way of bridging length and time scales, which is an alternative to the direct multi-scale models, where the simulated system is divided into regions of different length- and time-scales which are treated with different simulation techniques simultaneously³⁰. Instead of trying to combine the two, inherently very different simulation techniques, into one multi-scale modelling program, it is now possible to use the overlapping region to tune the larger scale model to the lower-scale one by direct comparison. This approach has the advantage that it preserves the uniqueness and the integrity of each of the models and avoids creating overcomplicated software codes with very restricted applicability. This approach also avoids the artifact of the interface between regions of different length- and time-scales existing in the direct multi-scale models³⁰.

Finally, the large-scale implementation of the MD-tuned FEM simulation on a typical 100 grain microstructure showed that GBS, by redistributing the load in the system, can produce stress localization several times higher than the background stress under external uniform load. These stress localization, under suitable conditions, may become nuclei for microcracking and void formation.

Acknowledgements

The work of V. Yamakov is sponsored through the cooperative agreement: NCC-1-02043 with the National Institute of Aerospace, and the work of D. Phillips is sponsored through contract: NAS1-00135 with Lockheed Martin Space Operations.

References

1. Langdon, T.G. (2000): "Identifying Creep Mechanisms at Low Stresses," *Mater. Sci. Eng.*, Vol. A283, pp. 266-273.
2. Wolf, D., Jaszczak, J.A. (1993): "Tailored Elastic Behavior of Multilayers Through Controlled Interface Structure," *Journal of Computer-Aided Materials Design*, Vol. 1, pp. 111-148.
3. Adams, J.B., Wolfer, W.G., Foiles, S.M. (1989): "Elastic Properties of Grain Boundaries in Cu and Their Relationship to Bulk Elastic Constants," *Phys. Rev. B*, Vol. 40, pp. 9479-9484.
4. Mishin, Y., Farkas, D., Mehl, M. J., Papaconstantopoulos, D.A. (1999): "Interatomic Potentials for Monoatomic Metals from Experimental Data and ab initio Calculations," *Phys. Rev. B*, Vol. 59, pp. 3393-3407.
5. Yamakov, V., Wolf, D., Salazar, M., Phillpot, S.R., and Gleiter, H. (2001): "Length-Scale Effects in the Nucleation of Extended Lattice Dislocations in Nanocrystalline Al by Molecular-Dynamics Simulation," *Acta Mater.*, Vol. 49, pp. 2713-2722.
6. Yamakov, V., Wolf, D., Phillpot, S.R., Gleiter, H. (2003): "Dislocation-Dislocation and Dislocation-Twin Reactions in Nanocrystalline Al by Molecular-Dynamics Simulation," *Acta Mater.*, Vol. 51, pp. 4135-4147.
7. Merkle, K.L. (1991): "High-Resolution Electron Microscopy of Interfaces in FCC Materials," *Ultramicroscopy*, Vol. 37, pp. 130-152.
8. Merkle, K. L., (1994): "Atomic Structure of Grain Boundaries," *J. Phys. Chem. Solids*, Vol. 55, pp. 991-1005.
9. Medlin, D.L., Foiles, S.M., Cohen, D. (2001): "A Dislocation-Based Description of Grain Boundary Dissociation: Application to a 90° $\langle 110 \rangle$ Tilt Boundary in Gold," *Acta Mater.*, Vol. 49, pp. 3689-3697.
10. Dahmen, U., Hetherington, J.D., O'Keefe, M.A., Westmacott, K.H., Mills, M.J., Daw, M.S., Vitek, V. (1990): "Atomic Structure of a $\Sigma 99$ Grain Boundary in Al: a Comparison Between Atomic-Resolution Observation and Pair-Potential and Embedded-Atom Simulations," *Phil. Mag. Lett.*, Vol. 62, pp. 327-335.
11. Wolf, D. (1990): "Structure-Energy Correlation for Grain Boundaries in F.C.C. Metals – III. Symmetrical Tilt Boundaries," *Acta Metal.*, Vol. 38, pp. 781-790.
12. Rittner, J.D., Seidman, D.N. (1996): "<110> Symmetric Tilt Grain-Boundary structures in FCC Metals with Low Stacking-Fault Energies," *Phys. Rev. B*, Vol. 54, pp. 6999-7015.
13. Nishitani, S.R., Ohgushi, S., Inoue, Y., Adachi, H. (2001): "Grain Boundary Energies of Al Simulated by Environment-Dependent Embedded Atom Method," *Mat. Sci. Eng.*, Vol. A309-310, pp. 490-494.

14. Yamakov, V., Wolf, D., Phillpot, S.R., Mukherjee, A.K., Gleiter, H. (2003): "Crossover in Hall-Petch behavior in Nanocrystalline Materials by Molecular-Dynamics Simulation," *Phil. Mag. Lett.* Vol. 83, pp. 385-393.
15. Yamakov, V., Wolf, D., Phillpot, S.R., Mukherjee, A.K., Gleiter, H. (2002): "Dislocation Processes in the Deformation of Nanocrystalline Al by Molecular-Dynamics Simulation," *Nature Materials*, Vol. 1, pp.45-48.
16. Yamakov, V., Wolf, D., Phillpot, S.R., Gleiter, H. (2002): "Deformation Twinning in Nanocrystalline Al by Molecular-Dynamics Simulation," *Acta Mater.*, Vol. 50, pp. 5005-5020.
17. Chen, M., Ma, E., Hemker, K.J., Sheng, H., Wang, Y., Cheng, X.. (2003): "Deformation Twinning in Nanocrystalline Al," *Science*, Vol. 300, pp. 1275-1277.
18. Liao, X.Z., Zhou, F, Lavernia, E.J, Srinivasan, S.G., Baskes, M.I., He, D.W., Zhu, Y.T., (2003): "Deformation Mechanism in Nanocrystalline Al: Partial Dislocation Slip," *Appl. Phys. Lett.*, Vol. 83, pp. 632-634.
19. Liao, X.Z., Zhou, F, Lavernia, E.J., He, D.W., Zhu, Y.T. (2003): "Deformation Twins in Nanocrystalline Al," *Appl. Phys. Lett.*, Vol. 83, pp. 5062-5064.
20. Parrinello, M., Rahman, A. (1981): "Polymorphic Transitions in Single Crystals; A New Molecular Dynamics Method," *J. Appl. Phys.*, Vol. 52, pp. 7182-7190.
21. Nose, S. (1984): "A Unified Formulation of the Constant Temperature Molecular Dynamics Method," *J. Chem. Phys.*, Vol. 81, pp. 511-519.
22. Schiotz, J., DiTolla, F.D., Jacobsen, K.W. (1998): "Softening of Nanocrystalline Metals at Very Small Grain Sizes," *Nature*, Vol. 391, pp. 561-563.
23. Ogata, S., Li, J. & Yip, S. (2002): "Ideal Pure Shear Strength of Aluminum and Copper," *Science*, Vol. 298, pp. 807-811.
24. Iesulauro, E. (2002): "Decohesion of Grain Boundaries in Statistical Representations of Aluminum Polycrystals," Cornell University Report No. 02-01.
25. Hirth, J.P., Lothe, J. (1992): *Theory of Dislocations*, 2nd Edition, John Wiley & Sons, Inc.
26. Tvergaard, V. and Hutchinson, J.W. (1992): "The Relation Between Crack Growth Resistance and Fracture Process Parameters in Elastic-Plastic Solids," *Journal of the Mechanics and Physics of Solids*, Vol. 40, pp. 1377-1397.
27. Klein, P. and Gao, H. (1998): "Crack Nucleation and Growth as Strain Localization in a Virtual-Bond Continuum," *Engineering Fracture Mechanics*, Vol. 61, pp. 21-48.
28. O'Rourke, J. (2001): *Computational Geometry in C*, 2nd Edition, Cambridge University Press.
29. Shobu, K., Tani, E., Watanabe, T. (1996): "Geometrical Study on the Inhomogeneous Deformation of Polycrystals due to Grain-Boundary Sliding," *Phil. Mag. A*, Vol. 74, pp. 957-964.
30. Tadmor, E. B., Phillips, R., Ortiz, M. (1996): "Mixed Atomistic and Continuum Models of Deformation in Solids," *Langmuir*, Vol. 12, pp. 4529-4534.